Numerical stability analysis of a large-scale delay system modeling a lateral semiconductor laser subject to optical feedback

Koen Verheyden, Kirk Green, and Dirk Roose
Department of Computer Science, KU Leuven, Celestijnenlaan 200A, 3001 Heverlee, Belgium
(Received 10 December 2003; published 23 March 2004)

This paper highlights the use of advanced numerical tools to study the stability of large-scale systems of delay differential equations (DDEs). Specifically, we consider a model describing a semiconductor laser subject to conventional optical feedback and lateral carrier diffusion. The symmetry of the governing rate equations allows external cavity mode solutions (ECMs) to be computed as steady state solutions. Using the software package DDE-BIFTOOL, branches of ECMs are computed as a function of varying feedback strength. The stability along these branches is computed by solving eigenvalue problems, the size of which is governed by a step-length heuristic. In this paper, we employ an improved heuristic which substantially reduces the size of these eigenvalue problems. This approach makes the stability analysis of large-scale systems of DDEs computationally feasible.

DOI: 10.1103/PhysRevE.69.036702 PACS number(s): 02.60.Lj, 02.30.Ks, 42.65.Sf, 42.55.Ah

I. INTRODUCTION

This paper deals with the numerical stability analysis of steady state solutions of a large-scale system of delay differential equations (DDEs) [1]. Specifically, we consider a model describing a semiconductor laser subject to conventional optical feedback (COF) and lateral carrier diffusion. The numerical stability and bifurcation analysis of small-scale and medium-scale systems of DDEs is possible using the software package DDE-BIFTOOL [2]. However, for large-scale systems, for example, discretized partial differential equations with delay, the standard algorithm used to compute stability with DDE-BIFTOOL can be prohibitively expensive. To overcome this problem, we employ a method that lowers the cost of computing the stability of steady state solutions in large-scale systems [3].

The bifurcation analysis of semiconductor lasers with feedback has been a driving motivation towards the development of advanced numerical tools for DDEs; see, for example, the work on phase-conjugate feedback in Refs. [4–6] and the work on COF in Refs. [7–9]. Based on a model derived by Lang and Kobayashi [10], semiconductor lasers with feedback are modeled by rate equations for the evolution of the complex electric field E and the carrier density within the semiconductor material N. Feedback or delay arises from reflection from an external device to the laser and can be used to provide stable operation for high resolution imaging techniques [11].

In this paper, we extend the COF laser model to include lateral carrier diffusion and a transverse variation of the pump current applied to the laser [12], namely, the pump current is ''on'' above a longitudinal stripe and ''off'' on either side. Hence the carrier density is now dependent on the transverse coordinate. This is possibly the simplest extension to the DDE modeling the COF laser. Note that more detailed models include the effects of transverse electric field diffraction [13], multistriped geometries [14], and thermal variations [15]. However, our choice of model provides an ideal test case for our numerical tools.

A model describing the effect of lateral carrier diffusion for a single-stripe geometry was derived in Ref. [12]. Here, the deterministic dynamics were studied. In particular, the presence of low frequency fluctuations [16], a cause of power dropouts, was shown. In this paper, we will investigate the effect of diffusion on another well-known phenomenon in the COF laser, that of external cavity modes (ECMs) or continuous-wave solutions [17]. In the case of COF, these solutions operate at a constant carrier density N, constant intensity $|E|^2$, and constant angular velocity b. In Ref. [7] a technique for analyzing these periodic solutions as steady state solutions using DDE-BIFTOOL was developed. We will use the ideas presented in Ref. [7] to study the analogous steady state solutions of the COF laser subject to lateral carrier diffusion.

The paper is organized as follows. In Sec. II we introduce the advanced numerical tools we use. In Sec. III we introduce the rate equations describing the COF laser subject to lateral carrier diffusion and the ECM solutions. In Sec. IV we present a stability analysis of these ECMs. Finally, in Sec. V we draw conclusions and discuss future work.

II. NUMERICAL TOOLS FOR THE STABILITY ANALYSIS OF DDEs

In this section, we briefly describe how the stability of steady state solutions in systems of DDEs is computed. Section II A recalls the algorithm implemented in the standard version of DDE-BIFTOOL [2,18], while Sec. II B outlines our improved approach to the stability computation of large-scale systems of DDEs [3].

A. DDE-BIFTOOL

The software package DDE-BIFTOOL [2], for the numerical bifurcation analysis of DDEs, can treat equations with an arbitrary number of delays. For simplicity, we consider the case of a single delay; that is,

$$y'(t) = f(y(t), y(t-\theta)). \tag{1}$$

We are interested in the local stability of a steady state solution of Eq. (1). This is determined by considering the variational equation

$$y'(t) = A_0 y(t) + A_1 y(t-\theta) \tag{2}$$

around this steady state, where the Jacobians $A_0 := \partial f/\partial y(t)$ and $A_1 := \partial f/\partial y(t-\theta)$ are the derivatives of f with respect to the first and second variables. The spectrum is given by the roots of the characteristic equation,

$$\chi_1(\lambda) = \det(\lambda I - A_0 - A_1 e^{-\lambda\theta}). \tag{3}$$

We now briefly outline how the characteristic roots are computed; for further details see Ref. [18]. Solving the characteristic equation (3) by Newton's method requires good initial guesses of the roots, which are obtained as follows. Consider the linear map defined by one step of a linear multistep (LMS) method applied to Eq. (2). This map can be represented by a matrix whose size is a multiple of the size of the DDE system. The eigenvalues of this matrix correspond (by an exponential transform) to approximations of the rightmost characteristic roots. These approximate roots are subsequently corrected up to a desirable accuracy by Newton iterations on the characteristic equation (3).

The step length used in the LMS method determines the size of the eigenvalue problem. DDE-BIFTOOL implements a heuristic choice of the step length needed to approximate well all the roots with real part larger than a given constant $r \in \mathbb{R}$; that is, all roots that belong to the half plane $\mathsf{H}(r) := \{c \in \mathbb{C}: \mathrm{Re}(c) > r\}$. For this heuristic, the extent of the spectrum is estimated using $\|A_0\|$ and $\|A_1\|$. The size of the eigenvalue problem grows linearly with these norms. However, the use of $\|A_0\|$ and $\|A_1\|$ may lead to a severe overestimation of the spectrum in $\mathsf{H}(r)$, especially for large DDE systems; see Ref. [3]. Hence, a better choice of the step length can substantially reduce the computational cost.

B. An improved step-length heuristic

Our approach is based on two steps which we briefly discuss in the case of a single delay; for full details see Refs. [3,19].

First, a bounded subset that includes all roots that lie in the half plane $\mathsf{H}(r)$ is determined. Consider the roots of

$$\chi_2(\lambda) = \det(\lambda I - A_0 - A_1 e^{-r\theta - i\omega}). \tag{4}$$

If ω varies in $[0, 2\pi)$, these points form closed curves, which we denote by $\Omega(r\theta)$. We denote the "Ω regions" as the parts of the complex plane encircled by the curves $\Omega(r\theta)$. In Ref. [19] it is proven that each characteristic root in $\mathsf{H}(r)$ lies in one such Ω region. Instead of using $\|A_0\|$ and $\|A_1\|$, the improved step-length heuristic takes the size of $\Omega(r\theta) \cap \mathsf{H}(r)$ into account (generally a much smaller quantity). For a fixed $\omega \in [0, 2\pi)$, points on $\Omega(r\theta)$ are computed by solving Eq. (4) with fixed r, θ, and ω; that is, a linear (algebraic) eigenvalue problem, which has the size of the DDE system. Experiments indicate that only a few such eigenvalue problems (each corresponding to a fixed value of ω) must be solved to locate $\Omega(r\theta)$ accurately.

In the next step, approximations to the rightmost roots are obtained as in DDE-BIFTOOL. However, our approach uses a special-purpose LMS method [3], constructed in order to minimize the error in the approximated roots. This is the second reason why a larger step length can be used. Since the resulting eigenvalue problem is smaller, the total computational cost of the improved algorithm is smaller than that of DDE-BIFTOOL's standard algorithm.

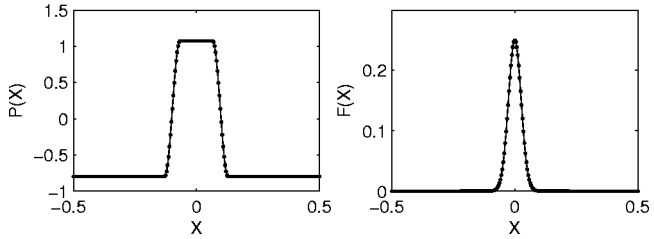

FIG. 1. Pump current profile $P(X)$ and spatial distribution of the electric field $F(X)$.

III. COF LASER SUBJECT TO LATERAL CARRIER DIFFUSION

The following model describes a longitudinally single-mode semiconductor laser subject to lateral carrier diffusion and weak COF,

$$\frac{dE(t)}{dt} = (1 - i\alpha)E(t)\zeta(t) + \eta E(t-\theta)e^{-i\phi}, \tag{5}$$

$$T\frac{\partial N(X,t)}{\partial t} = d\frac{\partial^2 N(X,t)}{\partial X^2} - N(X,t) + P(X) - F(X)[1 + 2N(X,t)]|E(t)|^2, \tag{6}$$

where $E(t) = E_x(t) + iE_y(t)$ is the complex electric field and $N(X,t)$ is the transversal carrier density. The given function $F(X)$ models the spatial distribution of the electric field. The transversal coordinate has been rescaled such that $X \in [-0.5, 0.5]$. Zero Neumann boundary conditions for the carrier density $N(X,t)$ are imposed at $X = \pm 0.5$. The time t is rescaled by the photon lifetime. Furthermore, the modal gain [20] is given as

$$\zeta(t) = \frac{\int_{-0.5}^{0.5} F(X)N(X,t)dX}{\int_{-\infty}^{\infty} F(X)dX}. \tag{7}$$

The rescaled pump current $P(X)$ has a maximum value of 1.075 (when on) and a minimum value of -0.8 (when off). The transversal parameters $F(X)$ and $P(X)$ determine the stripe structure of the laser. Specifically, $P(X)$ is modeled by a steplike function and $F(X)$ by a Gaussian function [12]; see Fig. 1. This single-stripe model can easily be adapted to describe a multistriped laser array by simple adjustments to the profiles of $P(X)$ and $F(X)$. Other parameters correspond to the linewidth enhancement factor $\alpha = 3$, the rescaled external cavity round-trip time $\theta = 1000$, the feedback phase $\phi = 0$, and the ratio of the carrier lifetime to the photon lifetime $T = 1000$. Furthermore, in the stability analysis of

Sec. IV we fix the value of the diffusion coefficient at $d = 1.68\times10^{-2}$ and consider the feedback strength η as our bifurcation parameter.

Physically, these parameters correspond to a semiconductor laser with a stripe width of 5 μm, pumped at 150 mA over the stripe and 0 mA either side of the stripe. The value of the diffusion coefficient corresponds to 3×10^{-4} m^2 s^{-1}, the carrier density at threshold is 4×10^8, the differential gain is 4000 s^{-1}, the photon lifetime is 1 ps, the electron lifetime time is 1 ns, and the external cavity is approximately 15 cm.

A. External cavity modes

Analogous to the COF laser, the ECM solutions of Eqs. (5) and (6) correspond to $E(t)\equiv A_s\exp(ib_st)$ and $N(t,X)\equiv N_s(X)$, where A_s and b_s are constants.

Of particular significance is the fact that Eqs. (5) and (6) exhibit symmetry in the transformation $(E,N)\rightarrow(cE,N)$, where $S^1=\{c\in\mathbb{C}||c|=1\}$ is the symmetry group [21]. Hence, ECMs are group orbits under this symmetry. In search of ECM solutions, we first rewrite Eqs. (5) and (6) in a rotating frame of reference [7]

$$E(t)=A(t)\exp(ibt). \tag{8}$$

Here, b is real and $A(t)=A_x(t)+iA_y(t)$ is complex. In this rotating frame of reference, Eqs. (5) and (6) become

$$\frac{dA(t)}{dt}=(1-i\alpha)A(t)\zeta(t)+\eta A(t-\theta)e^{-i\phi}-ibA(t), \tag{9}$$

$$T\frac{\partial N(X,t)}{\partial t}=d\frac{\partial^2N(X,t)}{\partial X^2}-N(X,t)+P(X) -F(X)[1+2N(X,t)]|A(t)|^2. \tag{10}$$

The ECMs can be calculated as steady state solutions of Eqs. (9) and (10) for certain values of b. These values b_s are solutions of the following transcendental equation, obtained by equating real and imaginary parts of the right-hand side of Eq. (9),

$$b_s+\eta\sqrt{(1+\alpha^2)}\sin(\phi+b_s\theta-\arctan\alpha)=0. \tag{11}$$

For computational purposes, the S^1 symmetry has to be resolved by fixing an isolated value of the electric field along the group orbit. This is obtained by imposing an extra algebraic constraint. In Ref. [7] the scalar condition $A_y=0$ was used. This condition has the numerical disadvantage that A_x and A_y are not of the same order of magnitude. Therefore, we use the condition that $A_x=A_y$.

B. Spatial discretization

To numerically investigate the above system we must first discretize Eq. (10). We use a second-order central difference formula on a uniform mesh, with ℓ intervals, over half the transverse length; that is, over $X\in[0,0.5]$. Hence at $X=0$,

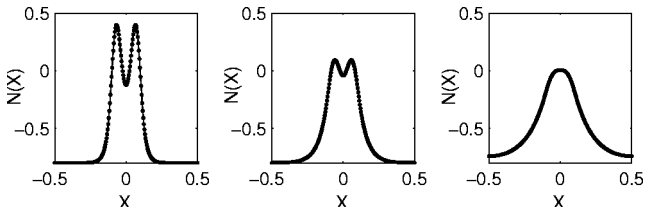

FIG. 2. Steady state profiles of the carrier density $N(X)$ computed for, from left to right, $d=6.72\times10^{-4}$, $d=3.25\times10^{-3}$, and $d=1.68\times10^{-2}$. (The intensities $|A|^2$ are 7.97, 7.69, and 3.33, respectively.) The hole burning is shown to be eliminated as d is increased.

zero Neumann boundary conditions are imposed. This gives a constant step size in space of $\Delta X=0.5/\ell$. The resulting DDE has size $\ell+3$; that is, A_x and A_y are real scalars, while N is a real vector of length $\ell+1$. Note that P and F are also vectors of length $\ell+1$. To approximate the modal gain [see Eq. (7)] we use the trapezoidal quadrature rule.

In Sec. IV, we use $\ell=128$ subintervals and, hence, the resulting DDE has size $n=131$. Note that this large-scale DDE has to be augmented with the unknown b [see Eq. (8)] and the extra condition $A_x=A_y$. Hence, we solve a nonlinear system for the scalars A_x, A_y, and b and the vector N.

IV. RESULTS

We compute ECM solutions of the COF laser with lateral carrier diffusion using the numerical procedure outlined above. Figure 2 shows carrier density profiles of ECMs of Eqs. (9) and (10) for varying values of the diffusion coefficient d. Note that for low values of d an effect associated with the carrier diffusion, known as optical hole burning, is observed [13]. This effect is eliminated as the value of d is increased.

After computing a steady state solution it can be followed as a parameter is varied using numerical continuation methods. Figure 3 shows a number of branches of steady state solutions computed using DDE-BIFTOOL. Plotted is the intensity $|A|^2$ against the feedback η, for the fixed value of $d=1.68\times10^{-2}$. Using the technique outlined in Sec. II we can accurately compute stability along these branches. Stable solutions are drawn as a solid line, unstable solutions as a broken line.

As is the case for the COF laser, our analysis shows that, for the most part, one stable steady state solution and one unstable steady state solution are born in saddle-node bifurcations ($\times$) (leftmost limit points of each branch), with the stable steady state solution destabilized in a Hopf bifurcation (*). The exceptions to this are the stable steady state solution born at the onset of feedback η and saddle-node bifurcations in which two unstable steady state solutions are born. Other Hopf bifurcations of unstable steady states are also marked. Hopf bifurcation points are characterized by a pair of purely imaginary roots of the characteristic equation, and are responsible for the onset of periodic pulses in the laser output. However, computing such periodic solutions is very expensive and beyond the scope of this paper; see Ref. [22].

We now focus on the branch of steady state solutions born

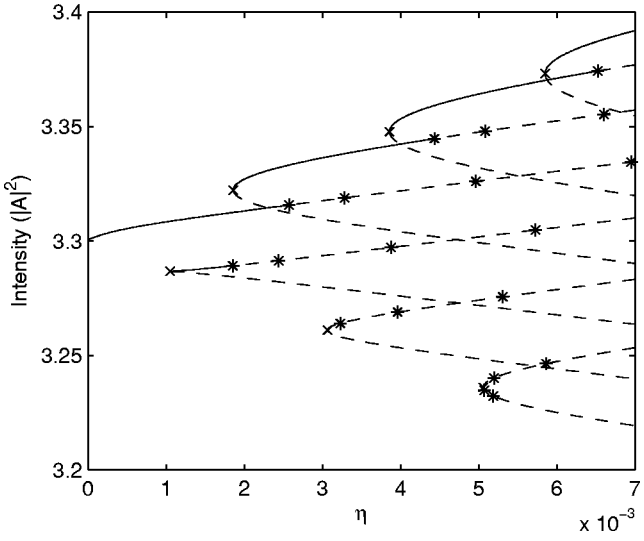

FIG. 3. Bifurcation diagram obtained by continuation with DDE-BIFTOOL showing the intensity of steady state solutions vs feedback strength η. Stable solutions are drawn as a solid line, unstable solutions as a broken line. Saddle-node bifurcations are denoted by ($\times$), Hopf bifurcations by (*).

in the saddle-node bifurcation ($\times$) at $\eta \approx 1.86 \times 10^{-3}$. The stable part of this branch is destabilized in a Hopf bifurcation (*) at $\eta \approx 4.45 \times 10^{-3}$. Using DDE-BIFTOOL we can accurately locate this Hopf bifurcation point. Figure 4 shows the computed spectrum for this point. Note that due to the S^1 symmetry of Eqs. (9) and (10) we always find an additional eigenvalue at zero. The step length used in the special-purpose LMS method is chosen such that the eigenvalues of the resulting matrix (by an exponential transform) are very good approximations to the roots of the characteristic equation for $\mathrm{Re}(\lambda) > -1$. This is indeed the case, as can be seen from the excellent agreement between the approximate roots ($+$) and the corrected roots after Newton iterations ($\bigcirc$).

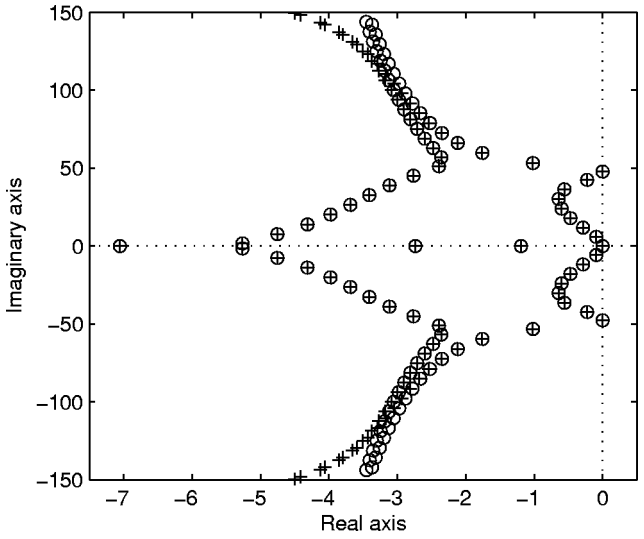

FIG. 4. Spectrum for the Hopf bifurcation point at $\eta \approx 4.45 \times 10^{-3}$. The approximated roots are marked by ($+$) and their corrections by Newton iterations by ($\bigcirc$).

Figure 4 shows that many more roots are approximated well by solving the eigenvalue problem, exceptions being those roots far from the origin.

To obtain Fig. 4 we used DDE-BIFTOOL with the improved step-length heuristic; this resulted in an eigenvalue problem of dimension $M = 6550$. Although large, this is feasible on current desktop computers. If one were to employ the standard heuristic used by DDE-BIFTOOL, an eigenvalue problem of dimension $M = 947\,916$ should be solved; this is computationally intractable.

In general, the dimension of the eigenvalue value problems used to calculate the Hopf bifurcation points in Fig. 3 varied between $M = 6550$ and $M = 8384$. While for the saddle-node bifurcation points the dimension of the eigenvalue value problems ranged from $M = 917$ to $M = 7336$, for increasing η. For all bifurcation points, the dimension of the eigenvalue value problem using the standard heuristic in DDE-BIFTOOL was $M \approx 948\,000$.

V. CONCLUSIONS

We have shown how advanced numerical methods can be used to analyze the steady state stability of large-scale systems of DDEs. Specifically, we have used DDE-BIFTOOL alongside a technique to compute the stability of a large-scale DDE modeling a semiconductor laser with COF and subject to lateral carrier diffusion.

After exploiting the symmetry of the governing rate equations, we computed branches of steady state solutions (ECMs) as a function of varying feedback strength. We computed stability along these branches by solving eigenvalue problems, the size of which are governed by a heuristic step length. In particular, an improved heuristic was shown to reduce the size of the eigenvalue problem substantially. In general, this makes the stability analysis of large-scale DDEs computationally feasible.

It should be noted that this single-stripe geometry is also present in semiconductor lasers with saturable absorbers [23]. There the laser is modeled by ordinary differential equations for the evolution of the carrier density on the stripe and on either side, and the photon number. The laser was shown to be excitable and self-pulsating solutions were found. For future work, an investigation of the periodic solutions of the COF laser with lateral carrier diffusion may reveal similar results.

Furthermore, this paper showcases the use and development of numerical tools for the study of stability in large-scale systems of DDEs.

ACKNOWLEDGMENTS

The authors would like to thank Thomas Erneux and Cristina Masoller for helpful discussions. This research presents results of the Project IUAP P5/22 funded by the program on Interuniversity Poles of Attraction, initiated by the Belgian State, Prime Minister's Office for Science, Technology and Culture. K.V. acknowledges support from the Fund of Scientific Research–Flanders (Belgium).

[1] J. K. Hale and S. M. Verduyn Lunel, *Introduction to Functional Differential Equations*, Applied Mathematical Sciences Vol. 99 (Springer-Verlag, Berlin, 1993).
[2] K. Engelborghs, T. Luzyanina, and D. Roose, ACM Trans. Math. Softw. **28**, 1 (2002).
[3] K. Verheyden, T. Luzyanina, and D. Roose, KU Leuven. Technical Report No. TW-383, 2003 (unpublished).
[4] K. Green and B. Krauskopf, Int. J. Bifurcation Chaos Appl. Sci. Eng. **13**, 2589 (2003).
[5] K. Green, B. Krauskopf, and K. Engelborghs, Physica D **173**, 114 (2002).
[6] K. Green, B. Krauskopf, and G. Samaey, SIAM J. Dynamical Systems **2**, 254 (2003).
[7] B. Haegeman, K. Engelborghs, D. Roose, D. Pieroux, and T. Erneux, Phys. Rev. E **66**, 046216 (2002).
[8] D. Pieroux, T. Erneux, B. Haegeman, K. Engelborghs, and D. Roose, Phys. Rev. Lett. **87**, 193901 (2001).
[9] D. Pieroux, T. Erneux, T. Luzyanina, and K. Engelborghs, Phys. Rev. E **63**, 036211 (2001).
[10] R. Lang and K. Kobayashi, IEEE J. Quantum Electron. **16**, 347 (1980).
[11] E. Lacot, R. Day, and F. Stoeckel, Phys. Rev. A **64**, 043815 (2001).
[12] M.S. Torre, C. Masoller, N.B. Abraham, and H.F. Ranea-Sandoval, J. Opt. B: Quantum Semiclassical Opt. **2**, 563 (2000).
[13] M. Münkel, F. Kaiser, and O. Hess, Int. J. Bifurcation Chaos Appl. Sci. Eng. **8**, 951 (1998).
[14] M. Münkel, F. Kaiser, and O. Hess, Phys. Lett. A **222**, 67 (1996).
[15] J.V. Moloney, in *Nonlinear Laser Dynamics: Concepts, Mathematics, Physics, and Applications International Spring School*, edited by Bernd Krauskopf and Daan Lenstra, AIP Conf. Proc. 548 (AIP Melville, NY, 2000), p. 149.
[16] D. Lenstra, B.H. Verbeek, and A.J. den Boef, IEEE J. Quantum Electron. **21**, 674 (1985).
[17] G.H.M. Van Tartwijk and G.P. Agrawal, Prog. Quantum Electron. **22**, 43 (1998).
[18] K. Engelborghs and D. Roose, SIAM (Soc. Ind. Appl. Math.) J. Numer. Anal. **40**, 629 (2002).
[19] K. Verheyden, T. Luzyanina, and D. Roose, KU Leuven Technical Report No. TW-382, 2003 (unpublished).
[20] G. P. Agrawal and N. K. Dutta, *Semiconductor Lasers* (Van Nostrand Reinhold, New York, 1993).
[21] B. Krauskopf, G.H.M. Van Tartwijk, and G.R. Gray, Opt. Commun. **177**, 347 (2000).
[22] K. Verheyden and K. Lust, KU Leuven Technical Report No. TW-357, 2003 (unpublished).
[23] J.L.A. Dubbeldam and B. Krauskopf, Opt. Commun. **159**, 325 (1999).